

Article

Optimal Capacitor Placement in Wind Farms by Considering Harmonics Using Discrete Lightning Search Algorithm

Reza Sirjani

Department of Electrical and Electronic Engineering, Eastern Mediterranean University, 99628 Gazimagusa, Mersin 10, Turkey; reza.sirjani@emu.edu.tr; Tel.: +90-392-630-2197

Received: 7 August 2017; Accepted: 18 September 2017; Published: 20 September 2017

Abstract: Currently, many wind farms exist throughout the world and, in some cases, supply a significant portion of energy to networks. However, numerous uncertainties remain with respect to the amount of energy generated by wind turbines and other sophisticated operational aspects, such as voltage and reactive power management, which requires further development and consideration. To fix the problem of poor reactive power compensation in wind farms, optimal capacitor placement has been proposed in existing wind farms as a simple and relatively inexpensive method. However, the use of induction generators, transformers, and additional capacitors represent potential problems for the harmonics of a system and therefore must be taken into account at wind farms. The optimal location and size of capacitors at buses of an 80-MW wind farm were determined according to modelled wind speed, system equivalent circuits, and harmonics in order to minimize energy losses, optimize reactive power and reduce the management costs. The discrete version of the lightning search algorithm (DLSA) is a powerful and flexible nature-inspired optimization technique that was developed and implemented herein for optimal capacitor placement in wind farms. The obtained results are compared with the results of the genetic algorithm (GA) and the discrete harmony search algorithm (DHSA).

Keywords: wind farm; reactive power; capacitor; harmonics; lightning search algorithm

1. Introduction

Wind power plants are increasingly important sources of clean energy that have a minimal environmental impact. Many wind energy technologies have been explored, and numerous wind farms have been installed on existing energy networks. Due to unpredictable nature of wind energy and its dependency on environmental conditions, it is usually required to integrate various renewable energy sources to form a hybrid system to provide high-quality and sustainable energy. Several aspects should be considered to provide suitable strategies for the stability and control of hybrid power systems [1].

Determining the optimal operating point of the wind turbine that produces maximum energy is essential. Therefore, many attempts have been done throughout the years to develop a suitable controller for maximum power point tracking (MPPT) for wind energy systems. In [2], dynamic operation and control strategies for a microgrid hybrid wind/photovoltaic/fuel cell have been examined and the proposed algorithm successfully controlled voltage and power under different weather conditions. Another intelligent controller for MPPT has been proposed for a hybrid solar/wind/diesel-engine power system [3].

From the power system stability point of view, the wind turbine should be able to remain connected to the network during faults. This capability of wind turbines, which should be taken in account in designing wind turbine controller and protection system, is called the fault ride-through

(FRT) capability. On the other hand, fault current limiter (FCL) or fault current controller should be applied in the wind power plants to protect the entire system. A fault analysis method for unbalanced distribution networks is proposed in [4], and a novel unsymmetrical faults analysis technique with hybrid compensation for microgrid distribution systems is presented in [5]. An algorithm for ground fault analysis of microgrid distribution was also proposed in [6]. In order to improve the transient stability, reduce the power fluctuations, and voltage support in a hybrid offshore wind farm/seashore wave power farm system, an intelligent damping controller has been proposed for a static synchronous compensator [7].

The overall performance of wind power depends on the subsystems of power plants, including those for reactive power compensation and energy storage, as these latter two components maintain the energy stability given varying electrical loads [8]. Even though the latest technologies enable wind generators to directly inject or absorb reactive power from the distribution network, most currently installed wind turbines use an inductor generator without voltage regulation or the ability to absorb grid reactive power [9]. In the past several years, the squirrel cage rotor induction generator has been commonly offered by wind turbine manufacturers as a trusted and inexpensive alternative. Squirrel cage rotor induction generators serve as induction machines and have capacitor modules that function as reactive power compensators to correct for differences in power factors; however, local reactive power compensation is unable to minimize the power losses and maximize bus voltages at levels that are satisfactory for many current wind farm owners [10].

Two different strategies have been proposed in the literature to fix the problem of poor reactive power compensation in wind farms. A single compensation center may be installed, based on a centralized approach, whereas a distributed approach may rely on compensation at each bus of a wind farm [11–13]. Optimal capacitor placement in existing wind farms represents a distributed approach for partially compensating for reactive power in order to minimize energy losses and to optimize the cost of reactive power management [9]. This method is simple and relatively inexpensive, and can be implemented after wind farms have already been established.

Clear benefits result from using capacitors to fix operational problems in different aspects of energy distribution systems; however, because of the complexity in finding the best location and size of these devices in networks, many research studies have focused on optimal capacitor placement. One comparative study on the optimal placement of shunt capacitors in energy distribution systems detailed several of the previously used methods for solving this problem, including analytical methods, numerical programming methods, heuristics methods, artificial intelligent methods, and multi-dimensional problems [14]. Another comprehensive review of heuristic optimization techniques proposed from 2001 to 2011 for optimal capacitor placement was presented in [15].

Further studies on optimal capacitor placement have been carried out in recent years, and new hybrid approaches, as well as new constraints, have been considered in the literature. In [16], a sensitivity index was first formulated to identify the most critical and suitable nodes for capacitor placement based on improvements in the voltage profile and the reductions in power loss. In the second stage, a combined fuzzy and GA-based approach was applied to determine the optimal size of capacitors, to improve the power factor, to reduce the burden on the substation, to decrease power loss, and to minimize voltage deviation in the distribution network. In [17], to overcome slow convergence, a hybrid optimization method based on the Harmony Search Algorithm (HSA) and the Particle Artificial Bee Colony algorithm (PABC) was proposed for optimal capacitor placement. The objectives were to minimize power loss and to improve the voltage profile in radial distribution networks. In [18], to reduce power loss and to improve bus voltages in unbalanced power systems, an optimal reconfiguration of distribution systems and placement of capacitors were simultaneously solved through combining the Big Bang–Big Crunch algorithm and a fuzzy-based multi-objective programming method. In [19], the suitable nodes for capacitor installation were determined by calculating the voltage stability and loss sensitivity indexes. Then, the optimum size of capacitors at candidate nodes was calculated by the Bacterial Foraging Optimization Algorithm (BFOA), considering

the load variations from light to peak loads. In [20], to minimize power loss and voltage deviation, Particle Swarm Optimization (PSO) was applied to solve the capacitor allocation problem for a modified distribution network connected to wind energy. Because of the uncertainties in wind speed and poor reactive power compensation, the fitness cost function in the study was nonlinear, and appropriate mathematical tools were applied. The Whale Optimization Algorithm (WOA) [21] and the Shark Smell Optimization (SSO) algorithm [22] are two additional recently developed metaheuristic optimization techniques that have been used to solve the optimal capacitor problem in distribution networks.

Several additional approaches have also contemplated harmonics. In particular, the most important power quality problems in wind power plants stem from the variance in harmonics across a system; these problems must be seriously considered during energy management. For example, the power conductors in wind power plants have high switching frequencies. Also, many elements in wind farms, such as power cables, transformers, reactors, and capacitor banks have nonlinear behavior and can resonate with one another. Even so, the installation of additional shunt capacitors for partial reactive compensation will increase the nonlinearity of the system components and therefore make harmonic considerations inevitable. In [23], power quality constraints such as total harmonic distortion (THD) and maximum voltage deviation were taken into account to determine the optimum placement, size, and number of both switched and fixed capacitors. The multi-objective formulation was solved by the Non-Dominated Sorting Genetic Algorithm (NSGA-II), and tested on a practical example. In [24], transient switching overvoltages were examined as a novel approach in the process of deciding optimal capacitor placement in order to minimize losses and THD on a long-term horizon.

In the present work, we aimed to determine the best location and size of capacitors in an existing wind farm in order to support local reactive power compensation and to thereby minimize energy losses and total costs. We evaluated system equivalent circuits in two cases, either considering or disregarding harmonics, and also based our determinations on modelled wind speed and wind power generation. The most important components of hybrid power systems that are used for the efficient and flexible interconnection of renewable energy resources are electronic converters. In addition, several stable power sources, such as batteries, fuel cells, super-capacitors, or diesel generators, must be integrated into hybrid systems to supply sufficient and stable power [1]. These additional devices make a lot of technical challenges on the power quality of systems and capacitors may not be able to provide reactive power requirement. For this reason, the present paper only focuses on the existing wind farms and neglects the hybrid power systems.

In [9], optimal capacitor placement in an existing wind farms, has been proposed as a partial reactive power compensation approach. A genetic algorithm was applied to find a limited number of capacitors on different buses and the effect of harmonics was neglected. In the present paper, by considering the harmonic distortion in the system components, the equivalent circuit is modified. For the first time, total harmonic distortion after capacitor placement is controlled in the wind farms and harmonic power loss has been considered in energy loss calculations.

In particular, for the purposes of the present study, a discrete version of the lightning search algorithm (DLSA) is proposed and developed at following. Proposed in 2015, the lightning search algorithm (LSA) is a powerful and flexible optimization technique [25] that was inspired by the natural phenomenon of lightning. Some engineering optimization problems related to the parameter extraction of solar cell models [26], as well as modelling wind power [27], controlling voltage and frequency in a solar thermal power plant [28], and designing a speed controller for an induction motor drive [29], have been recently and successfully solved by applying the LSA method. The results obtained by the DLSA for the optimal placement of capacitors were compared with the results obtained by the genetic algorithm (GA), and the discrete harmony search algorithm (DHSA) at different wind speeds considering or disregarding harmonics. The results demonstrate the effectiveness of the DLSA method; this method showed a faster convergence and better convergence characteristics in comparison to other methods. DLSA is proposed for the first time to show the application of a novel discrete optimization technique in solving complex problems in large scale.

2. System Equivalent Circuit

As induction generators are widely used in wind farms, these must be first modelled in order to analyse the wind farm system. In practice, the stator resistance is negligible, and the induction generator per-phase equivalent circuit can be simplified, as shown in Figure 1, where s is the induction generator slip and V_1 is the generator input voltage. R_c and X_m are open circuit resistance and reactance, respectively. R_r and X_r are rotor resistance and reactance, respectively. X_s is stator reactance.

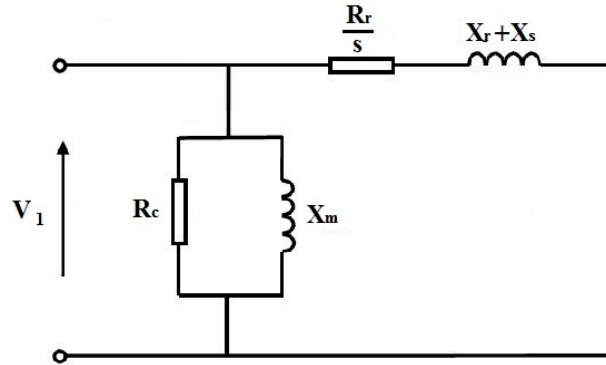


Figure 1. Approximated equivalent circuit of induction generator.

Considering the simplified equivalent circuit, we can compute the produced active power and the absorbed reactive power at bus j , as follows [9]:

$$P_j^{wind} - Q_j^{wind} = -|V_1|^2 \left(\frac{1}{R_c} + \frac{1}{j X_m} + \frac{1}{R_r/s - j (X_r + X_s)} \right) \tag{1}$$

$$Q_j^{wind} = P_j^{wind} \left(\frac{R_c}{X_m} \right) \left(\frac{s^2 (X_r + X_s) (X_m + X_r + X_s) - R_r^2}{s^2 (X_r + X_s)^2 - R_r^2 - s R_r R_c} \right) \tag{2}$$

The power injected at bus j is

$$P_j^{injected} = P_j^{wind} \tag{3}$$

$$Q_j^{injected} = -(Q_j^{wind} + Q_j^{compensated}) \tag{4}$$

where $Q_j^{compensated}$ is the reactive power compensated by bus j , including automatic compensation in the wind turbine and the additional shunt capacitor. In practice, for a range of wind speeds from 4 to 25 m/s, the active wind power generated at bus j can be approximated by

$$P_j^{wind}(v_j^{wind}) = \frac{P_{j, rated}^{wind}}{1 + \exp\left(\frac{v_j^{wind} - c1}{c2}\right)} \tag{5}$$

where v_j^{wind} is the wind speed at node j , $P_{j, rated}^{wind}$ is the rated value of the wind turbine at bus j , and the coefficients $c1$ and $c2$ are constants defined to minimise the approximation error [9].

By considering the harmonic distortion in the system, the per-phase equivalent circuit of any wind turbine connected to the electric distribution system in wind farms can be modelled as in Figure 2. In this circuit line feeder, the transformer, induction generator, and capacitor are modelled, and are connected to the network at each busbar. In this circuit, h is the harmonic order, which is defined as the ratio of frequency under analysis and the fundamental frequency [30].

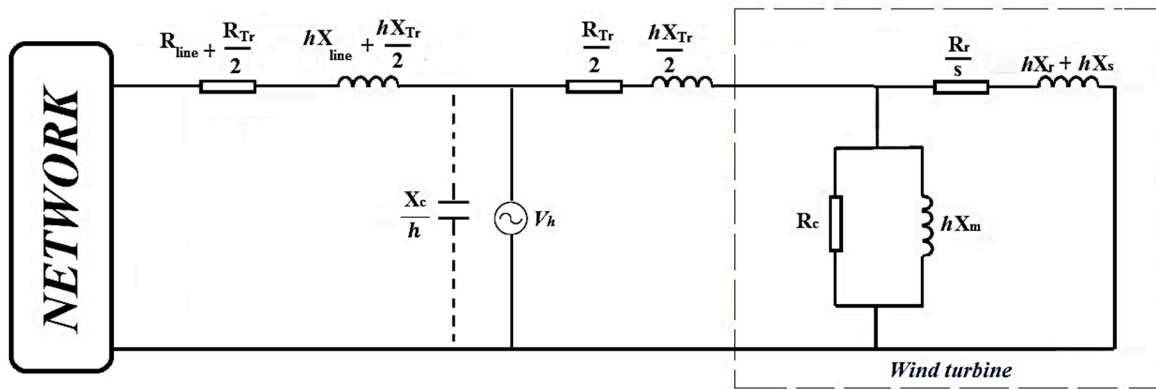


Figure 2. Per-phase equivalent circuit of each wind turbine considering harmonics.

The slip of the induction generator is a function of the harmonic frequency and is computed as follows [30]:

$$s_h = 1 - \frac{\omega_r}{h\omega_s} \tag{6}$$

where s_h is the wind turbine slip at the harmonic order of h , ω_s is the synchronous speed and ω_r is the generator rotor speed.

The system admittance is proportional to the harmonic current flowing in the system. A change to capacitor size will be reflected in the system admittance for different harmonic frequencies; this variance represents the central problem addressed in this study. Consequently, the harmonic currents, harmonic voltages, and the amount of harmonic distortion at each bus will be also be completely modified.

3. Problem Formulation

The aim of the present exploration is to determine the optimal placement and size of capacitors for instalment on different buses of an existing wind farm in order to minimise energy losses, total cost, and reactive power absorption in the external distribution system considering voltage limits and maximum permissible harmonic distortion. To define the objective function, apart from the additional capacitor banks, we suppose a basic capacitor module that includes connection, switch and control subsystems.

For this study, the following objective function F is considered.

$$F = \text{Minimise} \left\{ \sum_{k=1}^N X_e (\Delta E)_{loss,k} + \sum_{j=1}^M [K_j (X_b + X_a Q_j^c)] + Cost_{Q(total)} \right\} \tag{7}$$

where N represents the number of lines; M is the number of buses; $\Delta E_{loss,k}$ is energy loss per year at line k in $\$/(\text{kWh}/\text{year})$; Q_j^c is total reactive power at bus j in (kVar); and, $Cost_{Q(total)}$ is yearly cost of purchased reactive power by the grid operator in the case of insufficient reactive power compensation at the wind farm ($\$/\text{year}$); X_a and X_b are yearly depreciation of the installation and the maintenance costs, respectively, of basic modules and additional capacitor banks; and X_e is average price of the unsold energy. K_j is defined as a binary variable and is equal to 1 if a capacitor is present at bus j and to 0 if no capacitor is present.

The energy losses at each line are computed by

$$E_{loss,k} = \int_T P_{loss,k}(\tau) d\tau \quad (8)$$

where $P_{loss,k}$ is power loss at the k th line in kW and T is the duration. Total real power loss is defined by

$$P_{loss} = P_{loss}^{(Fund.)} + P_{loss}^{(harmonics)} \quad (9)$$

in which

$$P_{loss}^{(Fund.)} = \sum_{j=1}^M \frac{R_j (P_{tot,j}^2 + Q_{tot,j}^2)}{|V_j|^2} \quad (10)$$

$$P_{loss}^{(harmonics)} = \sum_{h=h_{min}}^{h_{max}} P_{loss}^{(h)} = \sum_{h=h_{min}}^{h_{max}} \sum_{j=1}^M R_j (I_j^{(h)})^2 \quad (11)$$

$P_{loss}^{(Fund.)}$ and $P_{loss}^{(harmonics)}$ are the fundamental and harmonic components of total power loss, respectively. V_j is the voltage at bus j . $P_{tot,j}$ and $Q_{tot,j}$ are the total active and reactive powers at bus j , respectively, and R_j is the resistance of branch j . $I_j^{(h)}$ is magnitude of the j th branch current for the h th harmonic order. h_{min} and h_{max} are the minimum and maximum harmonic orders, respectively.

The objective function is minimised by being subjected to constraints defined by the limits of voltage and harmonic distortion at each bus, which are given as follows:

$$V_{min} \leq |V_j| \leq V_{max} \quad (12)$$

$$THD_j(\%) \leq THD_{max}(\%) \quad (13)$$

where V_j is the voltage and $THD_j(\%)$ is the total harmonic distortion at j th bus.

The optimal capacitor placement problem is formulated as a nonlinear integer optimization problem by considering both the capacitor location and size as discrete variables. Radial power flow and harmonic power flow programs should be run more than five hundred times and it is a sophisticated and time-consuming procedure. Therefore, a robust and reliable optimization technique that can solve complex discrete problems in large scale must be developed to solve such a problem. The lightning search algorithm (LSA) is a powerful and flexible optimization technique without many initial parameters that has been applied for many engineering problems. It is a fast, reliable, and simple method and can be updated to binary or discrete versions [31].

4. Lightning Search Algorithm

The lightning search algorithm (LSA), proposed by Shareef et al. in 2015 [25], is based on the natural phenomenon of lightning. Similar to the other metaheuristics algorithms, the LSA needs a population to begin the search. The fast particles in the search are known as projectiles. The process is divided into three types of projectiles: transition, space, and lead projectiles.

Transition Projectile: An early stage formation of step leaders results from the ejection of the transition projectile in a random direction. This can be modelled as a random number using uniform probability distribution.

$$f(x^T) = \begin{cases} \frac{1}{b-a} & \text{for } a \leq x^T \leq b \\ 0 & \text{elsewhere} \end{cases} \quad (14)$$

where x^T represents the initial tip energy of the step leader. For a population of N step leaders (SL), wherein $SL = [sl_1, sl_2, sl_3, \dots, sl_N]$, N random projectiles $P^T = [p^T_1, p^T_2, p^T_3, \dots, p^T_N]$ that satisfy the solution dimensions are required.

Space Projectile: The space projectile enables the best leaders position to be reached by ionising the region of the previous leaders tip energy as step + 1, wherein step leaders are changed after N .

The space projectile P^S position = $[p^S_1, p^S_2, p^S_3, \dots, p^S_N]$ at step + 1 can be partially modelled as a random number generated from an exponential distribution using the shaping parameter μ , as follows:

$$f(x^S) = \begin{cases} \frac{1}{\mu} e^{\left(\frac{-x^S}{\mu}\right)} & \text{for } x^S \geq 0 \\ 0 & \text{for } x^S \leq 0 \end{cases} \quad (15)$$

The p^S_i at step + 1 can be represented at following:

$$p^S_{i-NEW} = p^S_i \pm \text{exprand}(\mu_i) \quad (16)$$

Only in situations where the projectile energy E^S_{p-i} is greater than the step leader E_{sl-i} can the path be extended and a good solution found; this guarantees new propagation or channel formation. If p^S_{i-NEW} offers a good solution in the next step, then the sl_i leader moves to another position, and p^S_i is updated to new p^S_{i-NEW} . Otherwise, p^S_i remains unchanged until the next step. If p^S_{i-NEW} becomes the lead projectile if it extends sl_{i-NEW} beyond the most recent extended leader during the process.

Lead Projectile: The lead step travels closest to the ground, as its projectile does not have enough potential for ionising large sections in front of the leader tip. This lead projectile can be expressed as a random number obtained from a normal distribution, as follows:

$$f(x^L) = \frac{1}{\sigma\sqrt{2\pi}} e^{\frac{-(x^L-\mu)^2}{2\sigma^2}} \quad (17)$$

The equation is defined by the shape parameter (μ) and is capable of investigating all of the directions from the current position of the lead projectile, which has a holding capacity represented by a scale parameter (σ). In the algorithm μ_L for the lead projectile, p^L is taken as p^L , and the scale parameter σ_L exponentially decreases as it moves closer to the ground or as it finds a better solution. p^L in step + 1 can be expressed as follows:

$$p^L_{NEW} = p^L + \text{normrand}(\mu_L, \sigma_L) \quad (18)$$

where *normrand* represents the random number generated by the normal distribution function. The new lead projectile p^L_{NEW} does not guarantee the spread of the leader step unless the lead projectile energy E^L_{p-i} is greater than the leader step projectile E_{sl-i} , which extends the algorithm to a satisfactory solution. If new p^L_{NEW} produces a good solution in next step, then the sl_i leader of the corresponding step is extended to a new sl_{L-NEW} position, and P^L is set to p^L_{NEW} . Otherwise, these remain unchanged until the next step, as in the case of the space projectile.

Another feature of LSA is its forking mechanism and channel elimination procedure. If the step leader energy is not sufficient after several trails, a channel appears for the successful step leader, and the unsuccessful leader is redistributed by channel time as the maximum trails number.

Discrete Lightning Search Algorithm (DLSA)

To update the conventional lightning search algorithm to a discrete version, we must first use a discrete uniform distribution to generate the initial solutions at the transition step before making any further modifications. The major difference between the two algorithms rests in the updating of the projectile position in the discrete algorithm. Therefore, unlike the LSA, the projectile position of the DLSA is expressed as a discrete vector. The following modifications should be applied to the standard LSA to convert it into a DSLA.

1. In Equation (14), the discrete uniform distribution should be used to generate discrete random values. The probability mass function graph of the discrete uniform distribution is shown in Figure 3.

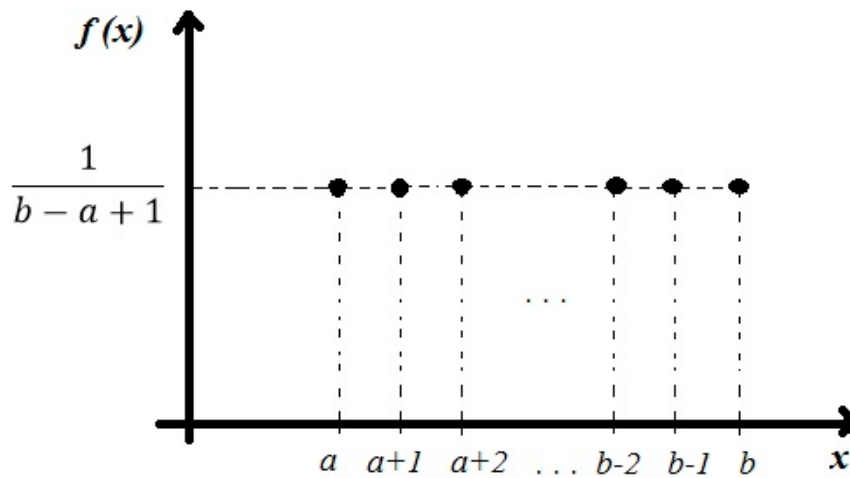


Figure 3. Probability mass function of discrete uniform distribution.

2. The probability function $T_f(p_i^S)$ should be used as represented in Equation (19) to map a discrete search space. Therefore, Equation (16) is modified to Equation (20) for the space projectile position at step + 1, which shows a decreasing probability of changing the position of the projectile for increasingly small spaces [31].

$$T_f(p_i^S) = \left| \tanh(p_i^S) \right| \quad (19)$$

$$p_{NEW,i}^S = \begin{cases} p_i^S + 1 & \text{if } r1 \leq T_f(p_i^S) \\ p_i^S - 1 & \text{otherwise} \end{cases} \quad (20)$$

3. Equation (18) should be modified to Equation (21) for the lead projectile position at step + 1.

$$p_{NEW}^L = \begin{cases} p^L + 1 & \text{if } r2 \leq 0.5 \\ p^L - 1 & \text{otherwise} \end{cases} \quad (21)$$

where $r1$ and $r2$ are random numbers.

The procedures applied in this study for calculating the power flow and the harmonic power flow in the distribution system are presented in detail in [32]. The procedures for the proposed DLSA method for optimal capacitor placement in wind farms considering harmonics are shown in Figure 4 as a flowchart.

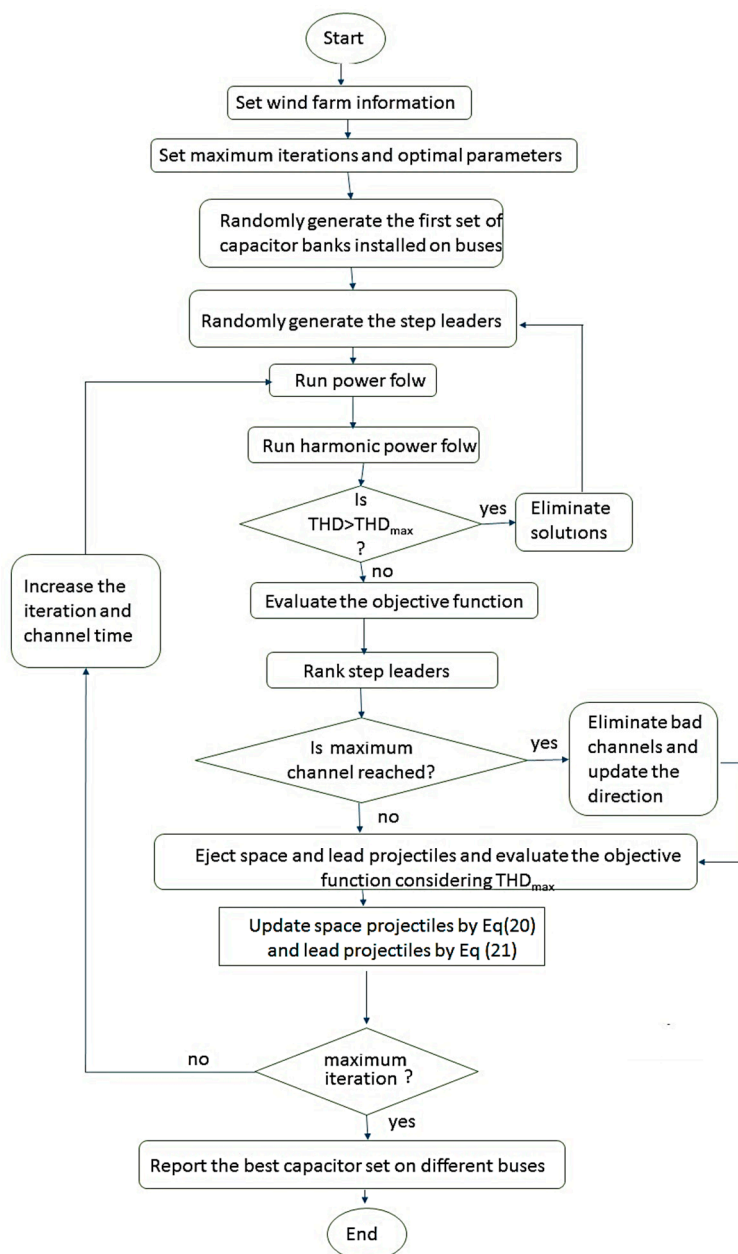


Figure 4. Flowchart of the proposed Discrete Lightning Search Algorithm (DLSA) method for optimal capacitor placement in wind farms considering harmonics.

5. Case Study and Results

This proposed method was implemented in a case study of an 80-MW wind farm in Kosovo using the “Shtime” project, as presented in [33]. The model of the distribution network is shown in Figure 5. The required data from wind turbine generators, wind turbine transformers, substation transformers, and cables are presented in detail in [33].

In the present wind farm system, 40 wind turbine generators, each rated at 2 MW, are individually connected to a 690-V bus that connects to the internal distribution network through 0.69/35 kV step-up transformers. The internal grid has eight sections with five wind turbines in each section. Within these sections, the wind turbines are connected through 35-kV underground cables of different lengths and capacities. In this study, assuming that the Transmission System Operator defines the voltage

limitations of the wind farm on the high voltage side, overvoltages on the distribution network are avoided. The voltage constraints in each bus are considered to range from 0.9 to 1.1 per unit.

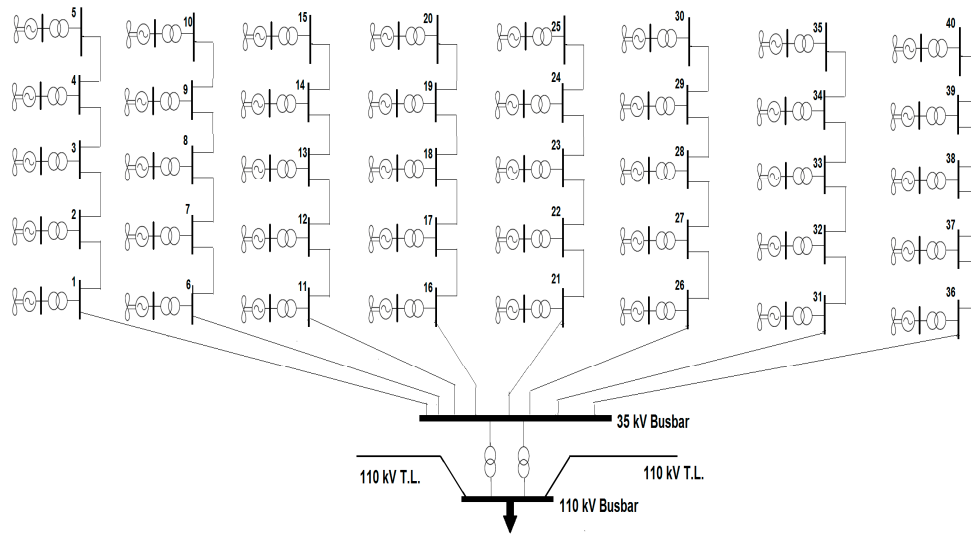


Figure 5. Model of 80 MW wind farm.

An automatic compensation system to compensate the reactive power absorbed by the wind turbine generators was considered in this study according to the operational scheme, as shown in Figure 6. According to Figure 7, specific amounts of reactive power, expressed as $Q_j^{Auto-comp}$, are injected to bus j per power factor correction and Var compensation, which depend on the wind power p_j^{wind} at that bus. This automatic compensation is definitely insufficient, for which additional support capacitors must be installed.

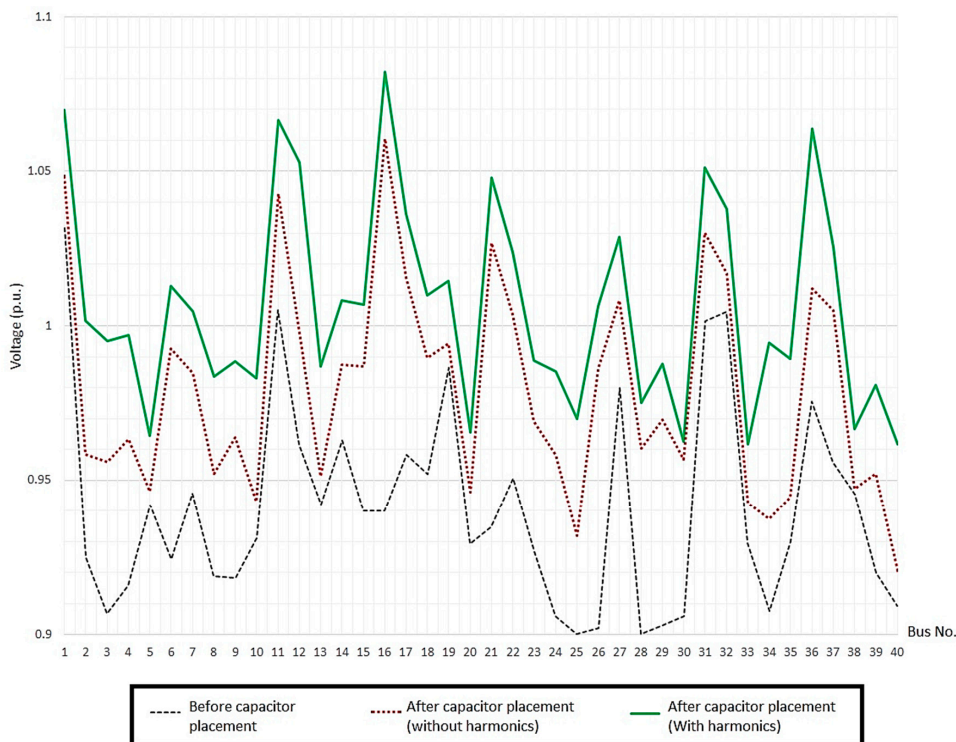


Figure 6. Comparison of the voltage profile before and after capacitor placement in wind farm.

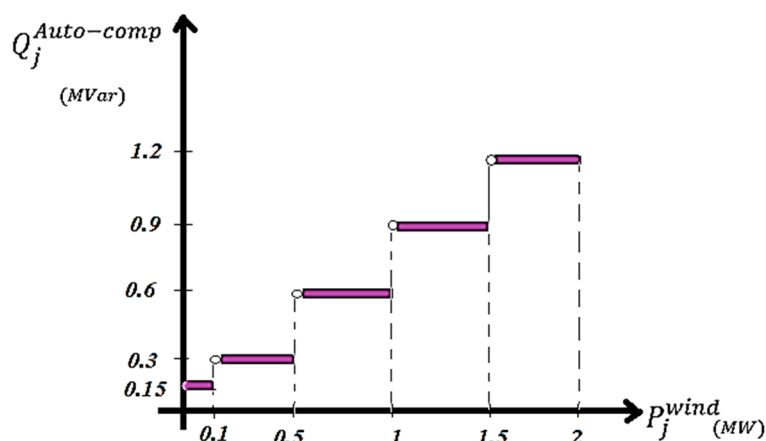


Figure 7. Graph of automatic reactive power compensation in wind generator.

According to site information, the wind speed of the region rarely exceeds 15 m/s. The automatic compensation is only acceptable for wind speeds of less than 8 m/s. Therefore, for this study, a necessary compensation based on wind speeds of 8 to 15 m/s was considered.

Assuming a life expectancy of five years, the yearly depreciations of X_a and X_b were estimated to be $X_a = \$1.1$ and $X_b = \$0.02$. The average price of unsold energy can then be used to estimate the cost of energy loss when considering that $X_c = 0.140$ \$/kWh. The investment cost of the first capacitor, including the cost of equipment and protection, is thus calculated to be \$1500. The selection of capacitor size is limited to the standard sizes of 150, 300, 450, 600, 750, 900, 1050, and 1200 kVar. The optimal size can be determined through a discrete optimisation for each bus so that $Q^c = N_c \times 150$ (kVar), wherein $N_c = 0, 1, \dots, 8$.

First, the proposed DLSA method was applied to the case system without considering harmonics. The results of optimal capacitor placement at different buses of the wind farm at distinct wind speeds is presented in Table 1. The maximum capacitor size to be installed at suitable buses is presented in the last column of Table 1, while the total size of the capacitors installed at all buses given different wind speeds is shown in the last row of Table 1. The value of the solution vector for some buses was zero, for which it would not be necessary to install capacitors at these buses.

Table 1. Results of optimal capacitor placement by DLSA without harmonics consideration.

Bus No.	Capacitor Size in (kVar) in Different Wind Speeds								Max. Q^c (kVar)
	8 m/s	9 m/s	10 m/s	11 m/s	12 m/s	13 m/s	14 m/s	15 m/s	
2	0	0	0	300	150	150	150	750	750
3	150	0	0	0	450	600	900	450	900
4	0	0	300	600	0	750	300	900	900
5	150	150	300	600	0	750	150	600	750
9	150	300	150	300	300	600	150	750	750
10	150	150	450	750	150	150	900	150	900
13	0	0	150	300	150	750	450	450	750
14	0	150	450	600	300	300	600	750	750
19	150	150	300	0	150	900	450	750	900
24	0	300	300	150	450	750	600	600	750
25	150	0	150	150	450	0	750	750	750
28	0	150	300	300	450	750	600	600	750
29	150	150	0	300	1200	600	150	1050	1200
30	300	450	0	150	450	150	1050	150	1050
34	150	150	0	300	750	750	1050	150	1050
35	300	300	450	600	600	750	900	1050	1050
39	150	300	150	600	750	600	1050	1200	1200
40	150	150	300	750	150	600	600	450	750
Total Q^c (kVar)	2100	2850	3750	6750	6900	9900	10,800	11,550	

Table 2 shows the results of optimal capacitor placement based on the DLSA. The total power loss and cost per distinct wind speeds according to radial power flow are compared with the results of three cases before capacitor placement, using the genetic algorithm (GA) as presented in [9], and the discrete harmony search algorithm (DHSA) as presented in [34]. As observed, the power loss and also the total cost at all considered wind speeds reduced significantly in comparison to before capacitor placement. Although an investment must be made to install additional capacitors, the total cost is proportional to the cost of power and energy losses; thus, a significant savings is obtained after capacitor placement. On the other hand, the results of the DLSA in terms of reduction in power loss and total costs appear to give lower figures than those calculated using GA and DSHA. Even so, the figures confirm the acceptable performance of the proposed DLSA in solving this problem.

Table 2. Comparison of different optimization techniques results without harmonic consideration.

Wind Speed (m/s)	Before Capacitor Placement		Using GA		Using DHSA		Using DLSA	
	Power Loss	Total Cost	Power Loss	Total Cost	Power Loss	Total Cost	Power Loss	Total Cost
	(MW)	(\$)	(MW)	(\$)	(MW)	(\$)	(MW)	(\$)
8	1.03	1,263,192	0.88	1,107,444	0.91	1,143,724	0.87	1,099,946
9	1.14	1,398,096	0.97	1,222,276	0.95	1,190,971	0.92	1,156,448
10	1.27	1,557,528	1.1	1,379,650	1.03	1,282,961	1.02	1,280,867
11	1.39	1,704,696	1.18	1,481,164	1.22	1,521,723	1.16	1,455,335
12	1.46	1,790,544	1.23	1,539,935	1.31	1,634,086	1.18	1,477,326
13	1.54	1,888,656	1.37	1,718,965	1.32	1,651,781	1.31	1,643,611
14	1.63	1,999,032	1.44	1,792,032	1.44	1,791,215	1.32	1,654,527
15	1.72	2,109,408	1.51	1,890,778	1.53	1,918,262	1.47	1,842,351

Based on the harmonic power flow presented in [32], the harmonic distortion of voltage in each bus after capacitor placement was calculated. As even and triplen harmonic orders are often not present in wind power plants; the harmonic orders $h = 5, 7, 11, 13, 17, 19,$ and 23 were considered, and the equivalent circuit in Figure 3 was applied. Table 3 shows the rate of total harmonic distortion at the different buses of the network. As can be observed, after capacitor placement, THD at most buses and at different wind speeds is quite high, so the harmonics problem appears to be significant and should not be ignored.

In considering the harmonics and defining the limitation for THD that the voltage of each bus should not exceed 5%, this problem was solved based on both radial power flow and harmonic power flow, and the results are shown in Table 4. If we compare the results of Tables 1 and 4, which disregard and consider harmonics, respectively, we find that the suitable buses for capacitor placement are quite different. Also, capacitor sizes at different wind speeds as well as the maximum capacitor size on each bus differ. The most important difference between the results of Tables 1 and 4 can be found in the last row, which shows the total capacitors installed on the system given differing wind speeds. These values are largely affected by the objective function. Upon considering harmonics, a greater total kVar is required, and larger capacitors must also be installed.

A comparison of the results for optimal capacitor placement in a wind farm according to three different optimisation techniques and the harmonics of the system are presented in Table 5. The total power loss in this case includes the two components of fundamental and harmonic power loss, as shown in Equation (9). For this reason, the power losses in Table 5 are higher than those in Table 2. Consequently, the total costs in Table 5 are greater than the total costs in Table 2.

Table 3. Total harmonic distortion (THD) of bus voltages after capacitor placement without harmonic consideration.

Bus No.	8 m/s	9 m/s	10 m/s	11 m/s	12 m/s	13 m/s	14 m/s	15 m/s
1	3.7%	7.8%	5.7%	5.6%	4.2%	10.5%	5.0%	5.6%
2	4.2%	3.0%	9.0%	3.0%	5.4%	9.0%	9.6%	8.7%
3	7.5%	3.6%	5.9%	10.5%	5.2%	7.4%	4.0%	8.1%
4	8.0%	5.5%	8.5%	8.2%	6.9%	7.0%	5.1%	8.0%
5	4.2%	8.0%	6.9%	6.1%	8.9%	3.0%	8.4%	10.7%
6	10.1%	4.0%	7.3%	10.2%	7.5%	10.7%	8.9%	10.1%
7	10.1%	7.7%	5.7%	6.3%	7.0%	8.9%	10.2%	8.1%
8	10.7%	7.2%	4.8%	10.7%	6.7%	7.6%	4.9%	6.2%
9	7.0%	3.9%	5.2%	8.6%	10.7%	9.1%	4.1%	8.7%
10	8.2%	8.4%	9.2%	5.9%	3.9%	7.6%	5.3%	3.5%
11	5.6%	8.9%	10.8%	6.7%	6.5%	7.4%	7.4%	4.5%
12	7.1%	9.2%	8.5%	8.2%	10.0%	10.6%	6.2%	3.1%
13	3.8%	8.7%	4.3%	8.8%	8.8%	6.6%	7.4%	10.9%
14	11.0%	6.6%	4.7%	7.7%	9.4%	9.0%	8.0%	10.3%
15	9.5%	5.7%	10.9%	10.8%	3.9%	9.5%	7.2%	5.6%
16	8.4%	4.2%	3.4%	6.7%	9.7%	5.4%	6.2%	3.2%
17	7.7%	8.9%	11.0%	5.9%	10.2%	3.2%	8.0%	5.1%
18	6.6%	7.8%	8.2%	11.0%	10.7%	6.7%	8.2%	9.5%
19	9.0%	6.9%	6.2%	6.9%	8.7%	3.7%	6.0%	10.6%
20	10.6%	4.8%	3.6%	7.1%	4.3%	8.2%	6.4%	5.2%
21	5.5%	9.7%	5.4%	5.2%	5.4%	5.4%	4.7%	10.2%
22	9.8%	6.7%	8.8%	7.0%	3.6%	4.7%	6.9%	8.7%
23	7.1%	4.1%	4.7%	4.6%	4.7%	5.9%	5.3%	8.4%
24	10.9%	8.4%	9.4%	10.8%	3.6%	4.4%	4.1%	10.2%
25	9.6%	9.1%	3.9%	3.1%	8.7%	8.5%	7.9%	8.6%
26	10.8%	8.6%	7.4%	4.2%	6.4%	4.4%	8.9%	7.5%
27	7.2%	10.5%	9.6%	4.1%	5.4%	5.5%	3.1%	4.3%
28	8.5%	8.3%	9.0%	5.2%	6.4%	4.2%	3.5%	7.7%
29	8.6%	8.4%	3.6%	4.1%	10.3%	8.8%	4.3%	6.7%
30	9.1%	11.0%	8.3%	7.3%	10.2%	3.3%	3.4%	7.6%
31	4.9%	9.5%	8.5%	8.6%	7.3%	5.4%	3.5%	3.5%
32	5.0%	4.8%	3.1%	6.6%	5.4%	3.8%	10.0%	4.9%
33	8.7%	5.2%	10.8%	9.8%	4.6%	4.5%	6.1%	7.6%
34	8.8%	10.2%	10.6%	10.4%	11.0%	4.8%	6.6%	9.0%
35	7.5%	7.7%	6.0%	8.4%	4.1%	8.5%	10.2%	5.0%
36	8.6%	3.2%	8.1%	5.5%	8.0%	10.0%	10.7%	6.3%
37	6.3%	5.1%	9.7%	10.6%	5.6%	3.9%	8.6%	9.8%
38	3.7%	3.3%	8.2%	4.9%	10.3%	3.5%	9.8%	10.6%
39	6.8%	4.9%	8.3%	6.7%	5.1%	9.3%	4.0%	4.8%
40	3.8%	5.0%	9.2%	3.3%	6.4%	9.8%	8.9%	3.4%

Table 4. Results of optimal capacitor placement by DLSA with harmonics consideration.

Bus No.	Capacitor Size in (kVar) in Different Wind Speeds								Max. Q^c (kVar)
	8 m/s	9 m/s	10 m/s	11 m/s	12 m/s	13 m/s	14 m/s	15 m/s	
3	0	0	300	150	300	750	150	600	750
4	0	150	0	600	750	750	300	450	750
5	300	300	300	150	1200	450	900	0	1200
8	0	0	150	150	0	900	900	600	900
10	450	300	0	450	900	0	1050	600	1050
13	0	150	300	300	150	150	300	750	750
14	0	0	300	450	150	600	750	0	750
15	150	300	300	450	150	1200	300	900	1200
18	0	0	0	300	150	300	600	750	750
19	0	150	300	300	150	300	750	600	750
20	150	150	450	450	750	600	150	600	750
24	0	150	0	300	750	600	300	750	750
25	300	300	450	750	300	150	900	750	900
30	150	300	600	0	450	450	900	450	900
35	150	150	450	600	300	300	450	1050	1050
39	300	150	300	300	300	450	600	750	750
40	300	600	600	150	300	600	1050	900	1050
Total Q^c (kVar)	2250	3150	4800	5850	7050	8550	10,350	10,500	

Table 5. Comparison of different optimization techniques results with harmonic consideration.

Wind Speed (m/s)	Before Capacitor Placement		Using GA		Using DHSA		Using DLSA	
	Power Loss	Total Cost	Power Loss	Total Cost	Power Loss	Total Cost	Power Loss	Total Cost
	(MW)	(\$)	(MW)	(\$)	(MW)	(\$)	(MW)	(\$)
8	1.32	1,618,848	1.12	1,396,210	1.16	1,452,947	1.07	1,335,065
9	1.51	1,851,864	1.3	1,614,968	1.29	1,603,905	1.27	1,580,542
10	1.64	2,011,296	1.42	1,766,515	1.43	1,780,871	1.36	1,700,711
11	1.78	2,182,992	1.6	1,986,794	1.5	1,866,758	1.43	1,786,689
12	1.89	2,317,896	1.64	2,040,819	1.66	2,072,863	1.53	1,907,149
13	1.97	2,416,008	1.76	2,186,432	1.65	2,055,592	1.6	1,992,963
14	2.06	2,526,384	1.71	2,138,110	1.86	2,311,989	1.69	2,103,628
15	2.18	2,673,552	1.93	2,402,713	1.84	2,290,124	1.81	2,260,569

Table 5 demonstrates that a consideration of harmonics can lead to optimal capacitor placement for reducing power loss and total costs, and that the results using DLSA are superior to those of the other optimisation techniques considered in this study. In addition, greater power and energy losses are evident upon considering harmonics, which will require larger capacitor sizes to mitigate losses; even so, total costs will be reduced and will lead to potentially significant savings. Although total cost, power loss, and total kVar installed on different buses increase under the abovementioned considerations, the *THD* of bus voltages was controlled to remain below 5%, as shown in Table 6. The effect of harmonic distortion was minimised, and these results are more reliable and practical.

Table 6. THD of bus voltages after capacitor placement with harmonic consideration.

Bus No.	8 m/s	9 m/s	10 m/s	11 m/s	12 m/s	13 m/s	14 m/s	15 m/s
1	4.8%	4.1%	4.2%	5.0%	4.8%	5.0%	4.6%	4.9%
2	3.9%	4.1%	5.0%	3.8%	4.2%	5.0%	5.0%	4.8%
3	4.4%	4.2%	4.3%	4.5%	3.9%	4.2%	5.0%	4.0%
4	4.4%	4.0%	3.9%	4.6%	4.7%	4.5%	4.5%	3.7%
5	4.3%	5.0%	4.4%	4.8%	4.3%	5.0%	4.4%	3.8%
6	4.9%	3.7%	5.0%	4.8%	5.0%	4.0%	4.6%	4.5%
7	4.4%	4.1%	4.4%	3.8%	3.8%	3.7%	5.0%	3.7%
8	4.7%	4.9%	4.1%	4.6%	4.5%	4.2%	5.0%	5.0%
9	4.7%	4.2%	4.6%	4.4%	4.5%	4.4%	3.9%	4.1%
10	4.5%	4.9%	4.3%	3.8%	4.8%	3.8%	3.9%	4.5%
11	4.3%	4.1%	4.8%	4.5%	4.7%	4.3%	4.5%	4.8%
12	4.6%	4.9%	4.4%	4.9%	4.6%	5.0%	4.6%	4.7%
13	4.1%	4.7%	4.3%	5.0%	3.8%	4.0%	4.3%	4.2%
14	4.1%	3.9%	4.1%	4.0%	5.0%	4.2%	3.9%	5.0%
15	3.8%	4.9%	5.0%	4.1%	4.8%	3.9%	4.4%	4.4%
16	4.1%	4.1%	4.8%	4.7%	4.5%	4.0%	3.9%	4.9%
17	4.8%	4.6%	4.7%	4.7%	4.7%	4.6%	4.7%	4.7%
18	4.2%	4.0%	4.4%	4.1%	3.9%	4.6%	4.8%	4.7%
19	4.5%	3.9%	4.9%	4.5%	5.0%	4.4%	4.6%	4.9%
20	3.7%	3.8%	3.9%	4.4%	4.4%	4.8%	4.7%	5.0%
21	3.7%	5.0%	4.7%	4.2%	3.8%	4.6%	4.7%	4.8%
22	4.0%	5.0%	4.0%	4.9%	5.0%	4.9%	4.7%	4.8%
23	4.1%	4.7%	4.4%	4.0%	5.0%	5.0%	3.8%	4.4%
24	4.6%	4.0%	3.8%	4.5%	3.9%	4.1%	4.4%	3.7%
25	4.6%	3.8%	4.1%	4.1%	4.2%	4.5%	4.4%	4.8%
26	4.4%	4.9%	3.8%	4.3%	4.4%	4.7%	4.7%	3.9%
27	5.0%	4.0%	4.7%	5.0%	3.9%	4.4%	4.3%	4.3%
28	3.7%	4.2%	3.9%	4.0%	3.7%	3.8%	4.1%	4.9%
29	4.3%	4.1%	4.0%	4.7%	4.7%	3.7%	4.7%	3.9%
30	4.0%	4.3%	4.0%	4.7%	4.8%	3.8%	4.7%	4.8%
31	4.7%	4.1%	3.8%	3.9%	3.8%	4.4%	4.2%	3.8%
32	5.0%	4.7%	5.0%	4.3%	4.1%	4.4%	4.3%	4.5%
33	5.0%	3.9%	4.2%	4.1%	4.2%	5.0%	4.0%	5.0%
34	3.8%	4.5%	5.0%	4.3%	3.9%	3.7%	4.4%	4.6%
35	5.0%	4.5%	4.2%	4.8%	5.0%	4.1%	3.8%	3.7%
36	4.5%	4.6%	4.4%	4.1%	4.6%	4.0%	4.4%	4.0%
37	3.9%	4.5%	4.6%	4.6%	4.4%	5.0%	4.3%	3.8%
38	4.8%	3.8%	5.0%	3.7%	4.3%	4.1%	3.8%	3.8%
39	3.8%	4.3%	4.3%	4.6%	4.1%	5.0%	4.8%	4.8%
40	3.8%	5.0%	4.6%	4.2%	5.0%	4.1%	4.4%	4.8%

In order to validate the results, the voltage profile of wind farm for 10 m/s wind speed is obtained and are shown in Figure 6. Three cases of before capacitor placement, after capacitor placement neglecting harmonics and after capacitor placement considering harmonics have been considered and all bus voltages are compared. Obviously, capacitor placement improves the voltage profile and the results of the proposed algorithm with considering harmonics are much better than the case without harmonic consideration.

The bus voltage imbalance ratio for three cases of before capacitor placement, after capacitor placement neglecting harmonics, and after capacitor placement considering harmonics, are computed and compared in Table 7. A lower value of voltage imbalance ratio shows a better balance in system and can be expressed by [35]:

$$\text{VUR (\%)} = \sum_{j=1}^M \text{Max} \left(\left| \frac{|V_j^{a-b}| - V_j^{\text{Average}}}{V_j^{\text{Average}}} \right|, \left| \frac{|V_j^{b-c}| - V_j^{\text{Average}}}{V_j^{\text{Average}}} \right|, \left| \frac{|V_j^{c-a}| - V_j^{\text{Average}}}{V_j^{\text{Average}}} \right| \right) \times 100\% \quad (22)$$

where VUR is the voltage imbalance ratio and V_j^{a-b} , V_j^{b-c} , V_j^{c-a} are three-phase line voltages of bus j . V_j^{Average} can be calculated as:

$$V_j^{\text{Average}} = \frac{V_j^{a-b} + V_j^{b-c} + V_j^{c-a}}{3} \quad (23)$$

For calculating any voltage in harmonic analysis, all harmonic orders should be included as:

$$V_j = \sqrt{\sum_{h=1}^H (V_j^h)^2} \quad (24)$$

Table 7. Comparison of the voltage imbalance ratio before and after capacitor placement in wind farm.

Wind Speed (m/s)	Before Capacitor Placement	After Capacitor Placement (Neglecting Harmonics)	After Capacitor Placement (Considering Harmonics)
	VUR (%)	VUR (%)	VUR (%)
8	5.08	3.03	2.81
9	6.99	3.58	3.03
10	10.80	3.76	3.43
11	10.85	4.86	4.37
12	11.06	4.51	4.38
13	11.55	4.70	4.59
14	12.53	5.73	5.28
15	13.96	6.60	5.83

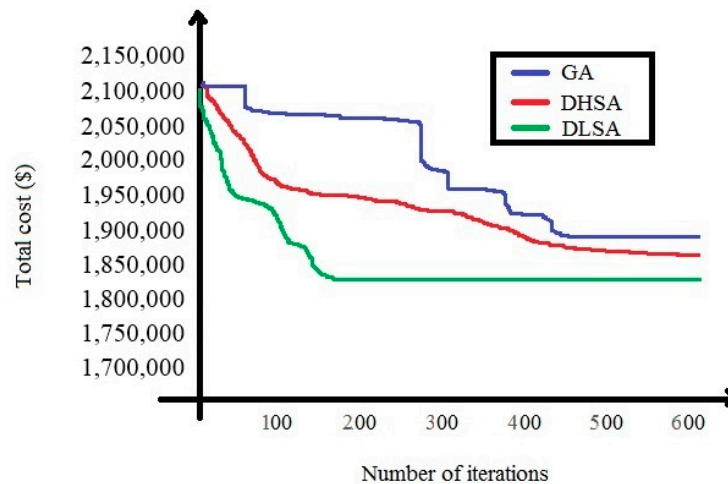
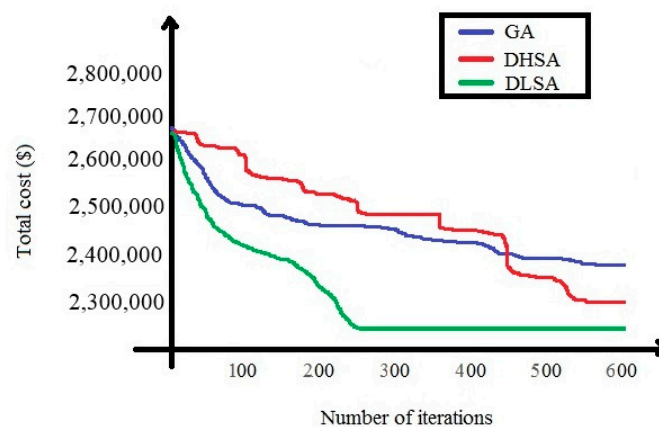
Table 7 shows that the total voltage imbalance ratios for all of the wind speeds have been significantly reduced after capacitor placement. In addition, the results of voltage imbalance ratio (VUR) reduction in the case of capacitor placement considering harmonics are better than the results of the case without harmonic consideration.

The most suitable optimal parameters that produce the lowest fitness function value with the best convergence were selected for all of the considered optimisation techniques and are shown in Table 8.

Finally, the convergence characteristics of all three optimisation techniques for determining optimal capacitor placement in a wind farm were evaluated at different wind speeds. Figures 8 and 9 compares the convergence characteristics of different methods either considering or disregarding harmonics at a wind speed of 15 m/s. As seen in both cases, the proposed DSLA has better performance, gives the lowest objective function and shows faster convergence.

Table 8. Optimal parameters for three different optimization techniques.

GA Optimal Parameters		DHSA Optimal Parameters		DLSA Optimal Parameters	
Mutation rate	0.02%	Minimum pitch adjusting rate	0.2	Maximum channel	5
Population size	40	Harmony memory size	40	Step leader size	40
Number of iterations	600	Number of iterations	600	Number of iterations	600

**Figure 8.** Convergence characteristics of different optimization techniques at 15 m/s wind speed without harmonic consideration.**Figure 9.** Convergence characteristics of different optimization techniques at 15 m/s wind speed considering harmonics.

6. Conclusions

Reactive power management is essential in wind farms. Many attempts have aimed to compensate for reactive power in this type of power plant. Although an automatic internal compensation occurs in wind turbines, the rate of reactive power compensation is not sufficient; for this reason, it is necessary to find a means of supporting local Var compensation. Optimal capacitor placement in an existing wind farm was proposed in the present study as an approach to partially compensate for reactive power loss and to thereby minimise energy losses and optimise the cost of reactive power management. However, an additional issue to take into account is that the installation of additional shun capacitors on buses with induction generators and transformers will increase the harmonic distortion in a system. The present study modelled wind power generation according to different wind speeds as well as the optimal placement and the size of capacitors upon considering or disregarding harmonics in

order to minimise total energy losses and costs. A discrete version of the lightning search algorithm (DLSA) was proposed and developed to solve this complex problem. To update the conventional lightning search algorithm to a discrete version, some modifications were made to provide discrete solutions and to update vectors. The results for an 80-MW wind farm showed that optimal capacitor placement can reduce power loss and total costs upon considering or disregarding harmonics. In the case of neglecting harmonics, the proposed capacitor placement method can reduce power loss by up to 19.2% and reduce the total cost up to 17.8%, which are much higher than the previous work in [9]. However, a consideration of harmonics will demonstrate greater power and energy losses and therefore lead to larger capacitor sizes; despite the higher total cost, the potential savings are still significant. By considering harmonics, the proposed method can reduce the total power loss and total cost up to 19.7% and 18.1%, respectively. The results also showed a significant reduction in the voltage imbalance ratio of buses after capacitor placement. Moreover, the results of using DLSA in all of the cases were superior to the results of other optimisation techniques such as GA and DHSA in terms of accuracy and speed. For the future work, the possibility of applying the proposed algorithm for hybrid systems with various constrains can be evaluated. The other devices such as static Var compensator (SVC), static synchronous compensator (STACOM), supercapacitor and automatic voltage regulator (AVR) can be considered and a comprehensive strategy for reactive power management in renewable energy systems may be proposed.

Conflicts of Interest: The author declares no conflict of interest.

Nomenclature

LSA	Lightning search algorithm
DLSA	Discrete lightning search algorithm
GA	Genetic algorithm
DHSA	Discrete harmony search algorithm
MPPT	Maximum power point tracking
FTR	Fault ride-through
FCL	Fault current limiter
HAS	Harmony Search Algorithm
PABCA	Particle Artificial Bee Colony algorithm
BFOA	Bacterial Foraging Optimization Algorithm
PSO	Particle Swarm Optimization
WOA	Whale Optimization Algorithm
SSO	Shark Smell Optimization
THD	Total harmonic distortion
NSGA-II	Non-Dominated Sorting Genetic Algorithm
R_c	open circuit resistance
X_m	open circuit reactance
X_s	stator reactance
R_r	rotor resistance
X_r	rotor reactance
$Q_j^{compensated}$	reactive power compensated by bus j ,
P_j^{wind} and Q_j^{wind}	produced active and reactive power at bus j
v_j^{wind}	wind speed at node j
$P_{j,rated}^{wind}$	the rated value of the wind turbine at bus j
$c1$ and $c2$	constants to minimise the approximation error
s_h	wind turbine slip at the harmonic order of h
ω_s	synchronous speed
ω_r	generator rotor speed

$\Delta E_{loss,k}$	energy loss per year at line k
Q_j^c	total reactive power at bus j
$Cost_{Q(tatal)}$	yearly cost of purchased reactive power by the grid
X_a and X_b	yearly depreciation of the installation and the maintenance costs
X_e	average price of the unsold energy
K_j	a binary variable
$P_{loss}^{(Fund.)}$	fundamental components of total power loss
$P_{loss}^{(harmonics)}$	harmonic components of total power loss.
V_j	voltage at bus j
$P_{tot,j}$ and $Q_{tot,j}$	total active and reactive powers at bus j
R_j	resistance of branch j .
$I_j^{(h)}$	magnitude of the j th branch current for the h th harmonic
h_{min} and h_{max}	the minimum and maximum harmonic orders
VUR	voltage imbalance ratio
$V_j^{a-b}, V_j^{b-c}, V_j^{c-a}$	three-phase line voltages of bus j
$V_j^{Average}$	average voltage along the phases
SL	The step leader
p^S	The space projectile
μ	shaping parameter
σ	scale parameter
$r1$ and $r2$	random numbers

References

1. Krishna, S.K.; Kumar, S.K. A review on hybrid renewable energy systems. *Renew. Sustain. Energy Rev.* **2015**, *52*, 907–916. [[CrossRef](#)]
2. Ou, T.C.; Hong, C.M. Dynamic operation and control of microgrid hybrid power systems. *Energy* **2014**, *66*, 314–323. [[CrossRef](#)]
3. Hong, C.M.; Ou, T.C.; Lu, K.H. Development of intelligent MPPT (maximum power point tracking) control for a grid-connected hybrid power generation system. *Energy* **2013**, *50*, 270–279. [[CrossRef](#)]
4. Lin, W.M.; Ou, T.C. Unbalanced distribution network fault analysis with hybrid compensation. *IET Gener. Transm. Distrib.* **2011**, *5*, 92–100. [[CrossRef](#)]
5. Ou, T.C. A novel unsymmetrical faults analysis for microgrid distribution systems. *Int. J. Electr. Power Energy Syst.* **2012**, *43*, 1017–1024. [[CrossRef](#)]
6. Ou, T.C. Ground fault current analysis with a direct building algorithm for microgrid distribution. *Int. J. Electr. Power Energy Syst.* **2013**, *53*, 867–875. [[CrossRef](#)]
7. Ou, T.C.; Lu, K.H.; Huang, C.J. Improvement of Transient Stability in a Hybrid Power Multi-System Using a Designed NIDC (Novel Intelligent Damping Controller). *Energies* **2017**, *10*, 488. [[CrossRef](#)]
8. Monteiro Pereira, R.M.; Machado Ferreira, C.M.; Maciel Barbosa, F.P. Reactive power management of a wind farm to prevent voltage collapse of an electric power system. In Proceedings of the 50th International Universities Power Engineering Conference (UPEC), Stoke-on-Trent, UK, 1–4 September 2015; pp. 1–5. [[CrossRef](#)]
9. Calderaro, V.; Galdi, V.; Piccolo, A.; Conio, G.; Fusco, R. Wind farm power plant: Optimal capacitor placement for reactive power compensation. In Proceedings of the IEEE PES ISGT Europe 2013, Lyngby, Denmark, 6–9 October 2013; pp. 1–5. [[CrossRef](#)]
10. Mesemanolis, A.; Mademlis, C.; Kioskeridis, I. High-Efficiency Control for a Wind Energy Conversion System with Induction Generator. *IEEE Trans. Energy Convers.* **2012**, *27*, 958–967. [[CrossRef](#)]
11. Pathak, A.K.; Sharma, M.P.; Bundele, M. A critical review of voltage and reactive power management of wind farms. *Renew. Sustain. Energy Rev.* **2015**, *51*, 460–471. [[CrossRef](#)]
12. Saqi, M.A.; Saleem, A.Z. Power-quality issues and the need for reactive-power compensation in the grid integration of wind power. *Renew. Sustain. Energy Rev.* **2015**, *43*, 51–64. [[CrossRef](#)]

13. Ahsan, S.; Siddiqui, A.S. Dynamic compensation of real and reactive power in wind farms using STATCOM. *Perspect. Sci.* **2016**, *8*, 519–521. [[CrossRef](#)]
14. Aman, M.M.; Jasmon, G.B.; Bakar, A.H.A.; Mokhlis, H.; Karimi, M. Optimum shunt capacitor placement in distribution system—A review and comparative study. *Renew. Sustain. Energy Rev.* **2014**, *30*, 429–439. [[CrossRef](#)]
15. Sirjani, R.; Mohamed, A.; Shareef, H. Heuristic optimization techniques to determine optimal capacitor placement and sizing in radial distribution networks: A comprehensive review. *Prz. Elektrotech.* **2012**, *88*, 1–7.
16. Gampa, S.R.; Das, D. Optimum placement of shunt capacitors in a radial distribution system for substation power factor improvement using fuzzy GA method. *Int. J. Electr. Power Energy Syst.* **2016**, *77*, 314–326. [[CrossRef](#)]
17. Muthukumar, K.; Jayalalitha, S. Optimal placement and sizing of distributed generators and shunt capacitors for power loss minimization in radial distribution networks using hybrid heuristic search optimization technique. *Int. J. Electr. Power Energy Syst.* **2016**, *76*, 299–319. [[CrossRef](#)]
18. Sedighzadeh, M.; Bakhtiary, R. Optimal multi-objective reconfiguration and capacitor placement of distribution systems with the Hybrid Big Bang–Big Crunch algorithm in the fuzzy framework. *Ain Shams Eng. J.* **2016**, *7*, 113–129. [[CrossRef](#)]
19. Devabalaji, K.R.; Ravi, K.; Kothari, D.P. Optimal location and sizing of capacitor placement in radial distribution system using Bacterial Foraging Optimization Algorithm. *Int. J. Electr. Power Energy Syst.* **2015**, *71*, 383–390. [[CrossRef](#)]
20. Ramadan, H.S.; Bendary, A.F.; Nagy, S. Particle swarm optimization algorithm for capacitor allocation problem in distribution systems with wind turbine generators. *Int. J. Electr. Power Energy Syst.* **2017**, *84*, 143–152. [[CrossRef](#)]
21. Prakash, D.B.; Lakshminarayana, C. Optimal siting of capacitors in radial distribution network using Whale Optimization Algorithm. *Alex. Eng. J.* **2016**. [[CrossRef](#)]
22. Gnanasekaran, N.; Chandramohan, S.; Sathish Kumar, P.; Mohamed Imran, A. Optimal placement of capacitors in radial distribution system using shark smell optimization algorithm. *Ain Shams Eng. J.* **2016**, *7*, 907–916. [[CrossRef](#)]
23. Azevedo, M.S.S.; Abril, I.P.; Leite, J.C.; de Medeiros, A.B. Capacitors placement by NSGA-II in distribution systems with non-linear loads. *Int. J. Electr. Power Energy Syst.* **2016**, *82*, 281–287. [[CrossRef](#)]
24. Javadi, M.S.; Esmaeel Nezhad, A.; Siano, P.; Shafie-khah, M.; Catalão, J.P.S. Shunt capacitor placement in radial distribution networks considering switching transients decision making approach. *Int. J. Electr. Power Energy Syst.* **2017**, *92*, 167–180. [[CrossRef](#)]
25. Shareef, H.; Ibrahim, A.A.; Mutlag, A.H. Lightning search algorithm. *Appl. Soft Comput.* **2015**, *36*, 315–333. [[CrossRef](#)]
26. Sirjani, R.; Shareef, H. Parameter Extraction of Solar Cell Models Using the Lightning Search Algorithm in Different Weather Conditions. *ASME J. Sol. Energy Eng.* **2016**, *138*, 041007. [[CrossRef](#)]
27. Sirjani, R.; Okonkwo, E.C. A new wind power model using the lightning search algorithm. In Proceedings of the 2016 HONET-ICT, Nicosia, Cyprus, 13–14 October 2016; pp. 93–97. [[CrossRef](#)]
28. Rajbongshi, R.; Saikia, L.C. Combined control of voltage and frequency of multi-area multisource system incorporating solar thermal power plant using LSA optimised classical controllers. *IET Gener. Transm. Distrib.* **2017**, *11*, 2489–2498. [[CrossRef](#)]
29. Abd Ali, J.; Hannan, M.A.; Mohamed, A. A Novel Quantum-Behaved Lightning Search Algorithm Approach to Improve the Fuzzy Logic Speed Controller for an Induction Motor Drive. *Energies* **2015**, *8*, 13112–13136. [[CrossRef](#)]
30. Preciado, V.; Madrigal, M.; Muljadi, E.; Gevorgian, V. Harmonics in a wind power plant. In Proceedings of the 2015 IEEE Power & Energy Society General Meeting, Denver, Colorado, 26–30 July 2015; pp. 1–5. [[CrossRef](#)]
31. Islam, M.M.; Shareef, H.; Mohamed, A.; Wahyudie, A. A binary variant of lightning search algorithm: BLSA. *Soft Comput.* **2017**, *21*, 2971–2990. [[CrossRef](#)]
32. Sirjani, R.; Bade, M.G. A global harmony search algorithm for finding optimal capacitor location and size in distribution networks. *J. Cent. South Univ.* **2015**, *22*, 1748–1761. [[CrossRef](#)]
33. Gashi, A.; Kabashi, G.; Kabashi, S.; Ahmetaj, S.; Veliu, V. Simulation the Wind Grid Code Requirements for Wind Farms Connection in Kosovo Transmission Grid. *Energy Power Eng.* **2012**, *4*, 482–495. [[CrossRef](#)]

34. Askarzadeh, A. A discrete chaotic harmony search-based simulated annealing algorithm for optimum design of PV/wind hybrid system. *Sol. Energy* **2013**, *97*, 93–101. [[CrossRef](#)]
35. Ou, T.C.; Su, W.F.; Liu, X.Z.; Huang, S.J.; Tai, T.Y. A Modified Bird-Mating Optimization with Hill-Climbing for Connection Decisions of Transformers. *Energies* **2016**, *9*, 671. [[CrossRef](#)]



© 2017 by the author. Licensee MDPI, Basel, Switzerland. This article is an open access article distributed under the terms and conditions of the Creative Commons Attribution (CC BY) license (<http://creativecommons.org/licenses/by/4.0/>).